The International Journal of **Medical Robotics** and **Computer Assisted Surgery**

THE INTERNATIONAL JOURNAL OF MEDICAL ROBOTICS AND COMPUTER ASSISTED SURGERY
Int J Med Robotics Comput Assist Surg 2011; **7**: 475–481.
Published online 7 October 2011 in Wiley Online Library (wileyonlinelibrary.com) **DOI:** 10.1002/rcs.431

ORIGINAL ARTICLE

A vision guided hybrid robotic prototype system for stereotactic surgery

Jun Wei[1,2]*
Tianmiao Wang[1]
Da Liu[1]

[1]*School of Mechanical Engineering and Automation, Beihang University, Beijing, China*

[2]*School of Control Science and Engineering, University of Jinan*

*Correspondence to: J. Wei, School of Control Science and Engineering, University of Jinan, Jinan, Shandong, China 250022.
E-mail: Cse_wj@ujn.edu.cn

Accepted: 8 August 2011

Abstract

Background Robot-assisted surgery (RAS) systems help surgeons performing accurate operations, but a number of drawbacks render them not yet suitable for clinical theaters and procedures. In this paper, a novel vision guided robotic system is proposed to facilitate navigation procedures.

Methods A vision guided hybrid robotic system is designed, consisting of a passive serial arm and an active parallel frame. Navigation is accomplished in three steps: approaching, aiming and insertion. First, the target is safely approached with the passive arm. Second, the trajectory is automatically aligned using the parallel frame. And then the target is reached by manual insertion. A stereo camera is used to position fiducials, the robot and the surgical tool. It also provides working area images for professional surgeons at a remote site.

Results The prototype system accomplished phantom and animal trials with satisfactory accuracy. The robot can easily be adjusted to avoid obstacles and quickly set up on an optimal 'approaching' place. The surgical tool is automatically aligned with the trajectory. The system can withdraw from the working area and restore the aiming posture freely. With the help of the working area images, some important navigation steps can be handled remotely.

Conclusions A novel vision guided robotic system is proposed and validated. It enables surgeons to fit the system to the clinical theater. System safety and feasibility are enhanced by multi-step navigation procedures and remote image monitoring. The system can be operated easily by general clinical staff.

Keywords robot-assisted surgery; stereo camera; hybrid robot; image registration

Introduction

Robotic surgery systems are designed to assist surgeons in carrying out a surgical procedure that may include the following steps: preoperative planning, intra-operative registration to pre-surgical plans, use of a combination of robotic assisted and manually controlled tools for carrying out the plan, and postoperative verification and follow-up (1). Since the early 1990s, many different systems have been developed and applied clinically. Neuromate has a six-DOF (degrees of freedom) robot arm to perform CT/MRI guided stereotactic neurosurgery. With the help of feedback control and multi-robot architecture, Robocast (2) can move more safely and perform brain surgery without damaging delicate brain tissue. ROBODOC (3) is a five- axis robotic system. Thanks to force and other safety sensors, it can perform hip surgery tasks

autonomously. Driven by low-powered motors in order to constrain movement to small regions, Acrobat (4) provides a guideline for the surgeon to avoid damaging healthy tissue during the operation. Spine assist (5) is a bone-mounted miniature robot in which a six-DOF parallel manipulator is used to assist spine surgery. PAKY (6) incorporates a two-DOF RCM (remote center of motion) and a Cartesian motion stage to position the target, also a passive arm is used for mounting the positioning module. The two rotary axes of RCM are parallel, and as a result the needle motion is restricted to a plane. B-Rob I (7) combines a four-DOF robot for gross positioning and a three-DOF NPU (needle positioning unit) for fine positioning. One NPU joint is used to move the needle vertically; the other two rotate the needle over a small range. Because of the workspace restriction on RCM and NPU, surgeons have to perform the gross positioning with great care. If the fine positioning module is not properly positioned, the navigation will have to be scrapped and restarted.

When surgeons enjoy the benefits of robot-assisted surgery, they have to face new challenges when using the robot; these include complex control operations, constrained working space and interference from the robot. Naturally, they prefer configuring the robotic system to be suitable for the clinical theater rather than changing the clinical theater to adapt to the robot. In this paper, we describe a vision guided robotic system to accomplish general guidance tasks. The system is designed to relax the limitations of using a robotic system and to shorten surgery time. Surgeons do not have to adapt to the robotic system; instead, they can easily configure and control the system, adapting it to the medical environment and procedures.

Materials and methods

System overview

The system consists of a hybrid robot, a stereo camera, registration markers, verification targets, a robot marker and a computer workstation, as shown in Figure 1. The hybrid robot includes a passive serial arm for manual gross positioning and an active parallel frame for automatic fine positioning. The stereo camera is used as a digitizer and provides working area images. The system procedure is designed to facilitate manipulation, provide check points, and support withdrawing and restoration of robot navigation. The navigation task is performed in the following steps:

- Fix the stereo camera at a suitable place where the working area is captured in its view.
- Position registration markers with the stereo camera and accomplish medical image registration on the workstation.
- Verify the registration accuracy by positioning the verification target- as if it was a designated target.
- Coarsely position the target with the passive robot, and track the parallel robot with the stereo camera.

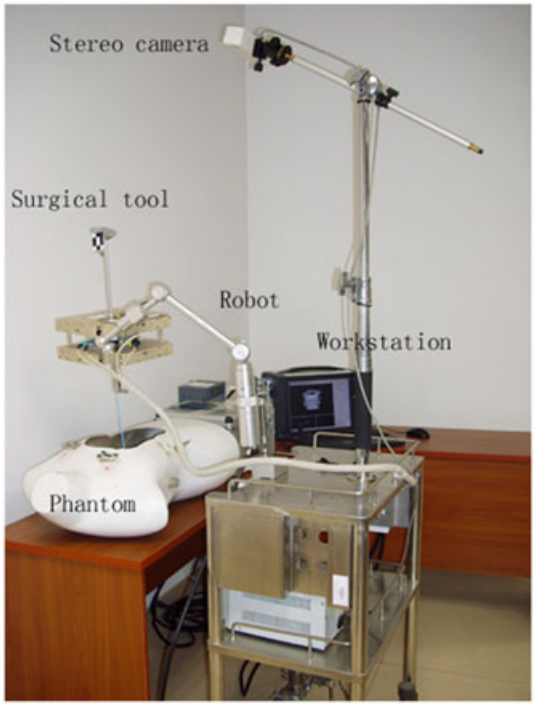

Figure 1. System structure on a phantom trial

- Lock the passive robot to retain posture when the system indicates that the target is reachable and when the robot is not obstructive to successive manipulation.
- Compute motion parameters and move the tool holders to aim at the target.
- Compute the insertion depth to reach the target, and manually insert the tool in the target.

Robot

The hybrid robot is composed of a passive serial arm and an active parallel frame as shown in Figure 2. The serial arm has five rotary joints. Its stretching length is 520 mm; the maximum length of a single link is 220 mm. In this study, we define the space points to be dexterous if they are reachable by the robot from 30%

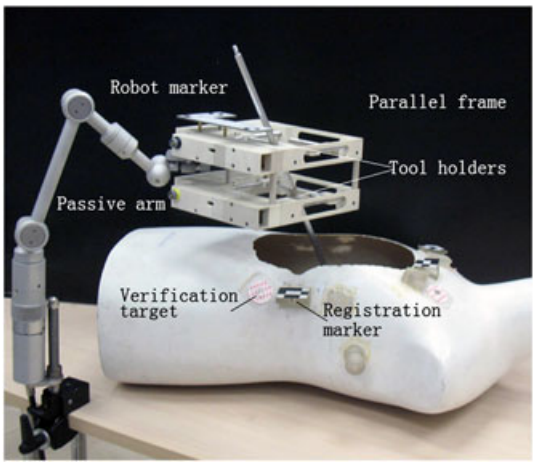

Figure 2. Hybrid robot on a phantom trial, showing the passive arm, parallel frame with marker, registration marker, and verification target. Stepping motors are embedded in the parallel frame

of all possible orientations. The serial arm has a workspace of $1040 \times 1040 \times 980\,mm^3$, where 91.1% is dexterous. The end effector of the passive arm can be moved around manually to accomplish the gross positioning task. There are hydraulic locking mechanisms (8) on each joint, and the joints can be locked and released by pressing a pedal. Compared with the active robot, the passive robot does not need motors and transmission mechanisms, more space is used to enhance its stiffness. Another prominent advantage of the passive robot is its safety and the facility to do gross positioning tasks in the clinical theater. There is no need for surgeons to worry about 'run-away' hazards, and it is unnecessary for surgeons to be familiar with the robot control. Surgeons focus only on dragging the robot to a posture compatible with the clinical theater. The passive serial arm can perform the guidance alone (9,10). However, it is inaccurate, time-consuming, and difficult to avoid obstacles.

The four-DOF parallel frame is designed for automatic tool alignment with the trajectory. It consists of two parallel-connected X–Y motion stages. There is one tool holder on each X–Y motion stage. One MCU (micro control unit) controls four stepping motors to drive the tool holders moving along ball-screws. The distance between the X–Y motion stages is 60 mm and the X/Y stroke is 80 mm. The parallel frame has a workspace of $310 \times 310 \times 220\,mm^3$, of which 68.9% is dexterous. The overall workspace of the hybrid robot is sufficient for neurosurgery and thoracic surgery. Because the tool can be moved inside X–Y motion stages, compared with PAKY and B-Rob I, the limitation on gross positioning is relaxed. The clinical staff can be more flexible in accomplishing the gross positioning task.

Stereo camera digitizer

The stereo camera positions fiducials, the robot and tool, providing working area images. MicronTracker is a commercially available stereo camera. It uses real-time stereoscopic vision to detect and track the pose of specially marked objects (11). However, some functions are not well supported by the MicronTracker, such as image compression, distance measurement on images, etc. We developed a customized digitizer based on the Bumblee2 camera from Ptgrey Company.

The digitizer consists of a Bumblee2 camera, markers, and a tool calibration template, as shown in Figure 3. The stereo camera collects images and transfers them to the workstation via a 1394 cable. We use X points to construct vision markers: an X point is an image corner formed by dark and light blocks arranged alternately around it as depicted in Figure 3. Algorithms are developed to find the X points and compute their 3D coordinates (12). Several X points constitute an image marker. Different markers identify different objects. The markers are recognized according to their geometric parameters. After positioning the markers, the images can be compressed and transferred to the remote workstation with the positioning results via a supervision network.

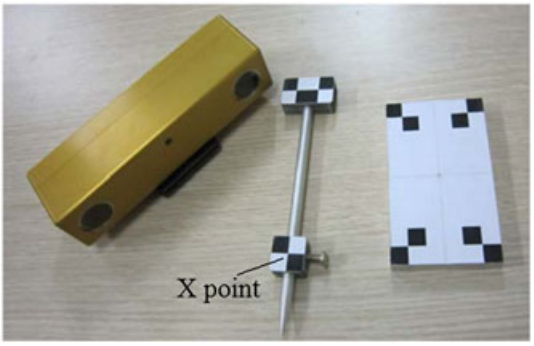

Figure 3. Stereo camera digitizer consisting of a stereo camera, markers and a tool calibration template

Image registration

In order to use medical images for navigation, the images need to be registered to the physical space (image-to-surgical-space registration). We use fiducials for registration. After positioning fiducials in the medical image space and the physical space, the space transformation matrix can be computed directly or by optimization algorithms. Probes are often used to position fiducials in physical space. This method introduces operating errors. In this system, the registration markers are designed to position fiducials in the camera space and the medical image. The registration fiducial is a porcelain ball planted into a registration marker, as shown in Figure 4, left. The markers can be stuck on a patient's skin.

A marker reference frame can be established based on the X points. We denote the coordinates of X points in the reference frame as A_r, B_r, C_r, and their corresponding coordinates positioned by the stereo camera as A_i, B_i, C_i. According to the right-handed coordinate system, a transformation matrix between the camera space and the marker reference frame can be computed. A fiducial is consequently positioned with its manufacture parameters and the transformation matrix.

The CT image of a fiducial marker is shown in Figure 4, right. After the surgeons outline an image region of a fiducial, the porcelain ball's image edge is automatically extracted with the SOBEL operator. And then its centroid $O_1(x_1, y_1)$ and radius r_1 are computed according to

$$C = \min \sum_{i=1}^{n} \left((r_i - x_1) + (c_i - y_1)^2 - r_1^2 \right)^2 \qquad (1)$$

where $(r_i, c_i)(i = 1, 2, \cdots, n)$ are the coordinates of the ith pixel on the edge.

Similarly, we can get another porcelain image centroid $O_2(x_2, y_2)$ and radius r_2. When the two images are on the same hemisphere, as shown in Figure 5, the fiducial position in the CT image O can be calculated as follows:

$$\begin{aligned} \overrightarrow{o} &= \overrightarrow{O_1} + \overrightarrow{O_1 O} \\ &= \overrightarrow{O_1} + \left(k^2 - r_1^2 + r_2^2\right) \times \overrightarrow{O_1 O_2} / 2k / \left\| \overrightarrow{O_1 O_2} \right\| \end{aligned} \qquad (2)$$

where k is the distance between the two images.

DOI: 10.1002/rcs

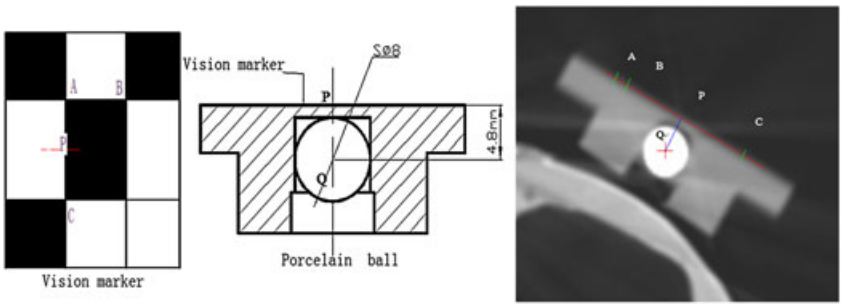

Figure 4. Registration marker. Left: CAD drawing of registration marker. Right: CT image of registration marker

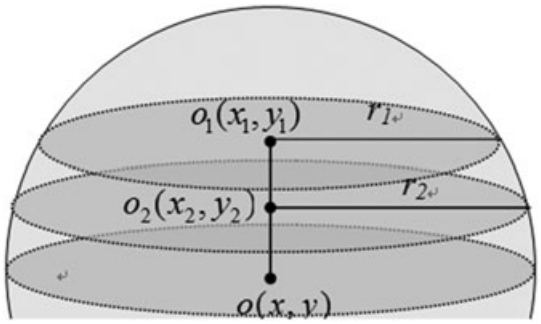

Figure 5. Diagram of positioning fiducial in CT image

Surgical planning and navigation

The medical image environment is developed based on VTK (Visualization ToolKit). The surgical plan defines a trajectory to reach the desired target. An Euler adjustment method is used to accomplish the surgical plan, as described by Wang (13). Navigation will proceed after medical image registration and surgical planning. The parallel robot and the surgical tool are tracked by the stereo camera during navigation, and are plotted in the 3D medical environment. In Figure 6, the plotted rectangles are X–Y motion stages of the parallel frame, the solid line is the tool, the dashed line is the designated trajectory, and the dots on the dashed line are the desired tool holder positions on the trajectory. The working room operator releases the passive robot joints, moves the parallel frame around until the planned trajectory is enclosed by the plotted rectangles. When the target is reachable, the operator will be indicated to lock the serial robot joints. After the surgeons finalize the plan and the navigation process, they can instruct the parallel frame to move the tool holders onto the planned trajectory. The tool will be mounted on holders, and manually inserted in the target. This operation is monitored by the stereo camera.

Tool calibration

To reach the target with the required accuracy, the tool must be calibrated to control the insertion depth. Tool calibration determines the tool tip offset S_p in the marker reference frame. Thereafter, the tool tip is positioned like a fiducial. Calibration is performed by putting the tool's tip onto a calibration template and rotating the tool around its tip, as shown in Figure 7. When the tool tip is put on the centroid of the calibration template, the U, V, W and the tip position S are acquired and recorded by the stereo camera. S_p can be computed according to

$$Q(x,y,z) = \min \sum_{i=1}^{n} \left| S(i) - {}^{c}_{p}T(i) \cdot S_p \right|^2 \qquad (3)$$

where $S(i)$ is the ith tip position acquired by the stereo camera, and ${}^{c}_{p}T(i)$ is the ith transformation matrix from the tool marker reference frame to the camera coordinate system.

Experiments

Phantom trials were conducted to test system accuracy and timing. Figure 8 shows a picture from a phantom trial. The phantom set-up is illustrated in Figure 6: six registration fiducials (RM) and a verification (VT) target were placed on the phantom surface, and the other three designated targets (DT) on a base inside the phantom. The

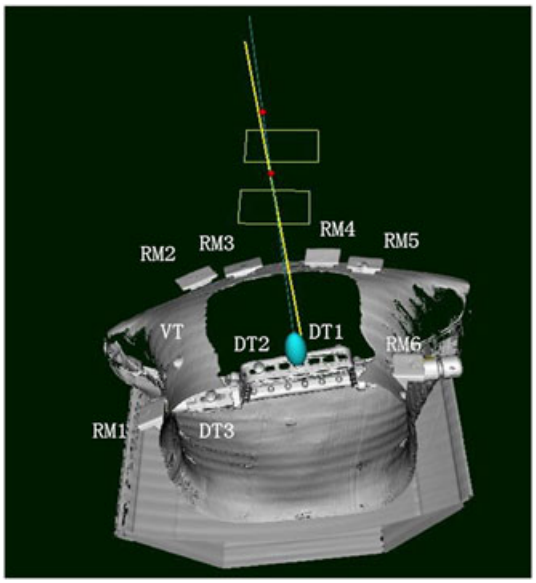

Figure 6. Phantom navigation in medical image space. RM1–RM6 are registration markers. DT1–DT3 are designated targets, VT is a verification target

DOI: 10.1002/rcs

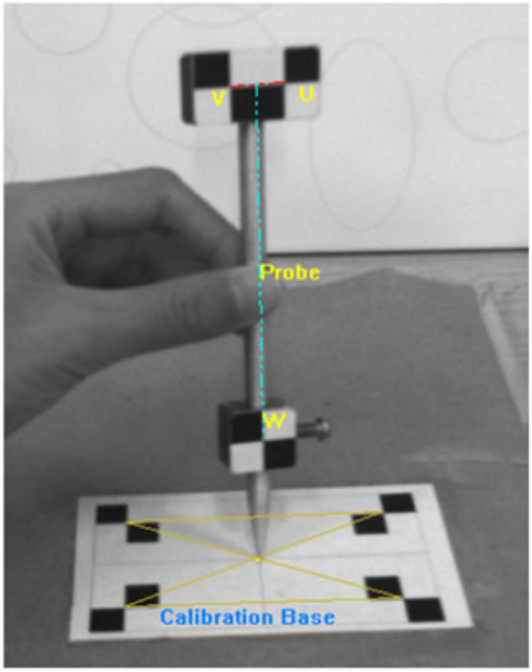

Figure 7. The tool is calibrated by rotating the tool around its tip. The tool tip is placed on the centroid of the calibration template

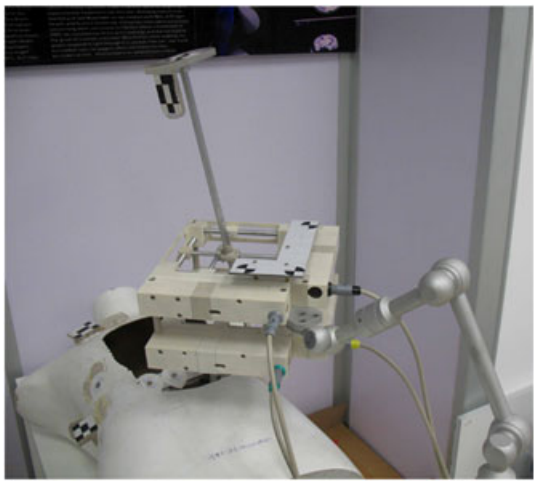

Figure 8. Phantom trial, showing the hybrid robot with marker, the tool with marker, the registration markers, and the verification target

targets were enclosed by fiducials. The registration fiducials were arranged to make the designated target as near as possible to their centroid. A target and a corresponding trajectory were first designated. Then the operator fixed the robot on a wheeled table and adjusted the stereo camera to accomplish image registration. The verification target was positioned to ensure registration accuracy. Thereafter, the operator approached the target using the robot with the camera tracking the robot. When the robot was approaching the target, the workstation continuously indicated whether the target was reachable. Based on the system's feedback, the operator chose a practical position and a robot posture, and then locked the passive robot joints. The surgeons at the remote site inspected the operations using the working area images and the 3D medical environment, and gave oral instructions. After the gross positioning, the posture of the robot and the trajectory of the tool were all finalized, the parallel frame moved the tool holders onto the designated trajectory. Then the tool was mounted and the surgeon performed the insertion procedure manually. The insertion depth is controlled by the surgeon manually, whereas the insertion orientation is autonomously managed by the parallel frame.

The phantom trial error was defined as the distance between the tool tip and the designated target, and was measured by feeler (thickness) gauges. In the case that the tool tip was obstructed by the target, the error was computed according to the actual insertion depth and the error measured by the gauges. The phantom trial results are listed in Table 1.

The system error consists of the camera, the image registration and the parallel frame errors. The position error of the X–Y motion stage is less than 0.02 mm. Because part of the tools (60–80 mm) is constrained between upper and lower X–Y motion stages, the parallel frame error can be controlled within 0.1 mm for a 300 mm insertion depth. This error will decrease as insertion depth is reduced. The image registration error is caused by position errors both in medical images and in physical space. Because the registration error is not easy to observe, the verification target is used to examine the registration result. The verification target is stuck near the incision. Compared with the designated target, it is further away from the centroid of the registration fiducials. According

Table 1. Results of the phantom trials

No.	Deviation (mm)	System preparation time (min)	Navigation and insertion time (min)
1	0.78	25	7
2	0.85	12	7
3	0.88	8	5
4	0.95	10	4
5	0.98	11	5
6	0.92	10	4

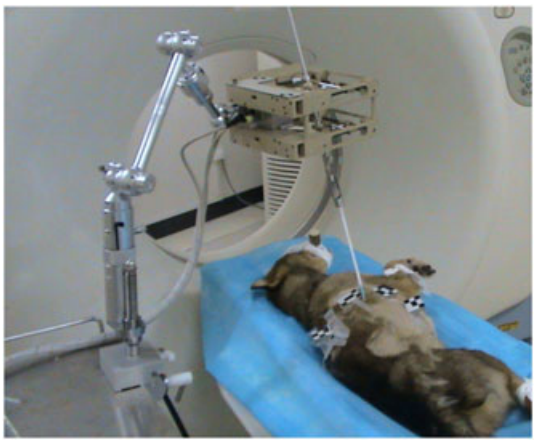

Figure 9. Animal trial. Pre- and post-surgery CT images were collected while the animal was static on the bed

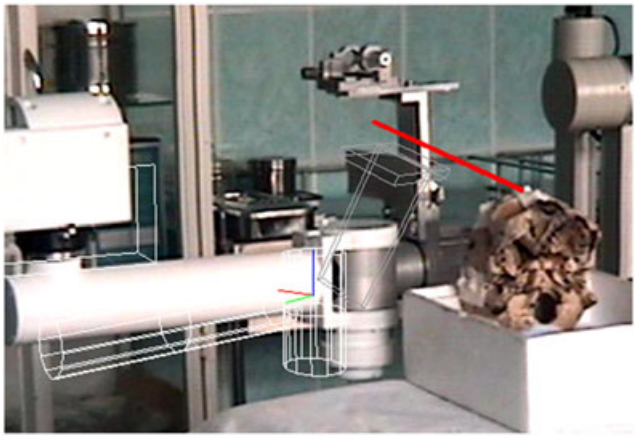

Figure 10. Robot simulation fused onto live working area image. The wireframe robot shows the robot motion. The tool is projected onto the live image to show the planned trajectory

to West (14), the error of the designated target will be smaller than the error of the verification target. In this study, the target error was often less than 1 mm when the error of the verification target was less than 1.75 mm.

Animal trials were conducted in lung argon-helium knife surgery, as shown in Figure 9. CT images were collected before and after the animal trials. In order to weaken the effects of breathing and minimize the difference between pre- and post-surgery CT images, the animals were overdose anesthetized. The animal trial error was defined as the distance between the target and the tool tip position in the post CT images. The animal trial errors were between 1.39 mm and 4.95 mm, with an average of 3.79 mm.

Results and discussion

There are engineering and economic problems to be solved in order to make robotic systems fit for medical use. It is better to use a compact, safe and simple operating robot in surgery. In this study, we use a five-DOF passive robot for gross positioning, a four-DOF parallel frame for fine positioning. The gross positioning is mainly conducted with the passive robot and partly with the parallel frame. Fine positioning is accomplished automatically to avoid time-consuming and unstable passive/semi-active manipulation. With the 'approaching–aiming–insertion' scheme, the navigation procedure can be performed conventionally, and the surgeons can thereby avoid complex robot control. Kinematics redundancy supports approaching the target optimally. Since the robot has a large dexterous space, the clinical staff can easily try suitable positions for the robot. The waist joint of the passive robot is locked separately, so that the system can be easily withdrawn from the working area, and the trajectory can be rapidly repeated during surgery. The system is sufficiently flexible for surgeons to plan surgery and arrange the clinical theater: surgery time is consequently shortened. The system successfully completed phantom and animal trials.

The stereo camera has some special advantages compared with other digitizers (infrared, magnetoelectric, etc.). Comprehensible images are helpful to improve the collaboration of clinical staff. The markers for the stereo camera are slimmer and cheaper. The working area images provide a new platform for procedure simulation. For example, the planned trajectory and the robot posture can be overlaid on the working area images for pre-operation evaluation, as shown in Figure 10.

This system architecture takes modular design into consideration. Different devices, such as a catheter motion device (15), can be attached to the passive robot to accomplish different tasks. It is possible to develop systems suitable for general purpose based on the hybrid modular architecture.

Acknowledgements

This study was supported by the Chinese National Science Fund for Distinguished Young Scholars (Grant No.60525314) and the Chinese International Science and Technology Cooperation Project (2006DFA12290). The authors would like to extend their gratitude to the anonymous reviewers and the following individuals for their helpful comments and suggestions: Suo Shan and Tao Shen.

References

1. Taylor RH, Stoianovici D. Medical robotics in computer-integrated surgery. *IEEE Trans Robot Autom* 2003; **19**(5): 765–781.
2. De Momi E, Cerveri P, Ferrigno G. Robot and sensors integration for computer assisted surgery and therapy (ICT-2007-215190-ROBOCAST). In *Proceedings of 14th International Conference on Advanced Robotics*, 2009; 1–6. Available at: http://ieeexplore.ieee.org/Xplore/login.jsp?url=http%3A%2F%2Fieeexplore.ieee.org%2Fiel5%2F5166725%2F5174665%2F05174751.pdf%3Farnumber%3D5174751&authDecision=-203
3. Bargar WL, Bauer A, Borner M. Primary and revision total hip replacement using the robodoc system. *Clin Orthop Relat Res* 1998; **354**: 81–94.

4. Jakopec M, Rodriguez y Baena F, Harris SJ, *et al*. The hands-on orthopaedic robot "Acrobot": early clinical trials of total knee replacement surgery. *IEEE Trans Robot Autom* 2003; **19**(5): 902–911.
5. Shoham M, Burman M, Zehavi E, *et al*. Bone-mounted miniature robot for surgical procedures: concept and clinical applications. *IEEE Trans Robot Autom* 2003; **19**(5): 893–901.
6. Fichtinger G, DeWeese TL, Patriciu A, *et al*. System for robotically assisted prostate biopsy and therapy with intraoperative CT guidance. *Acad Radiol* 2002; **9**(1): 60–74.
7. Kettenbach J, Kronreif G, Figl M, *et al*. Robot-assisted biopsy using ultrasound guidance: initial results from in vitro tests. *Eur Radiol* 2005; **15**: 765–771.
8. Liu D, Tang C. On hydraulically locking structure of robot joint for minimally invasive CT-guided surgery. *Robot* 2008; **30**(4): 298–303.
9. Taylor RH, Funda J, LaRose D, *et al*. A passive/active manipulation system for surgical augmentation. In Proceedings of 1st International.Workshop on Mechatronics in Medicine, Malaga, Spain, 1992.
10. Potamianos P, Davies BL, Hibberd RD. Intra-operative imaging guidance for keyhole surgery methodology and calibration. In Proceedings of 1st International Symposium on Medical Robotics and Computer Assisted Surgery, 1994; **1**: 98–104.
11. http://www.clarontech.com/platforms_microntracker.php, 2011, 9.
12. Wei J, Liu D, Wang TM, *et al*. Segment test based X corner detection and sub-pixel localization. *Robot* 2011; **33**(1): 97–101.
13. Wang LF, Huang YY, Wei J, *et al*. Operation planning approach of brain surgery robot system based on adjustment of Euler angle. *High Technol Lett* 2006; **16**(6): 596–599.
14. West JB, Fitzpatrick JM, Toms SA, *et al*. Fiducial point placement and the accuracy of point-based, rigid body registration. *Neurosurgery* 2001; **48**(4): 810–817.
15. Wang TM, Zhang DP, Liu D. Remote-controlled vascular interventional surgery robot. *Int J Med Robot Comput Assist Surg* 2010; **6**: 194–201.